Comparison of the Dynamic Behaviour between Bubbling and Circulating Fluidized Bed Combustors

Comparison of the Dynamic Behaviour between Bubbling and Circulating Fluidized Bed Combustors

Guillermo Martinez Castilla, Rubén M. Montañés, David Pallarès and Filip Johnsson

castilla@chalmers.se

Chalmers University of Technology, Energy Technology, Hörsalsvägen 7B, 412 96 Gothenburg, Sweden

Abstract

This work compares the dynamic behaviour of the flue gas side of large-scale bubbling and circulating fluidized bed (BFB and CFB respectively) boilers. For this, two dynamic models are developed and presented. The models are parametrized with design data from two industrial units and validated against steady-state operational data. The models are applied to investigate and compare the transient behaviour of BFB and CFB boilers of the same size given step changes in load and moisture content.

Results show that the heat transfer to the water walls in CFB units stabilizes faster, yielding smaller absolute changes in temperature once a new steady state is established. For these units, the presence of solids throughout the furnace makes the temperatures exhibit inverse responses before stabilization, whereas the BFB upper furnace is absent of such behaviour.

1. Introduction

Fluidized bed combustion (FBC) has become a favourite choice for thermal treatment of solid fuels since the 1970s and 1980s. Due to unique inherent strong mixing and heat transfer capabilities of the fluidized bed (FB) units, fuels of very different nature can be thermally converted in these boilers, ranging from different types of biomass to coal and municipal solid waste, as well as their mixtures. This allows FBC facilities to change fuels and co-fire mixtures of them depending on fuel price and availability. Furthermore, fluidized bed combustors are characterized by relatively low emissions through cost-efficient in-bed capture and reduction methods and high combustion and generation efficiency, what makes them crucial actors in many energy systems worldwide.

Depending on the fluidization velocity, fluidized bed combustors can be divided into bubbling and circulating fluidized beds (BFB and CFB, respectively). CFB units operate under conditions where a significant amount of solids is entrained by the gas, being externally recirculated into the riser through a cyclone and a loop seal preventing the gas to enter the cyclone from its leg. On the other hand, bubbling fluidized beds are operated at lower fluidization velocities so the amount of solids carried by the gas flow is not significant. These conceptual differences in both design and operation of FB boilers result in very different behaviours that need to be understood for an optimal design and operation of the boilers. Specially regarding heat transfer to the steam cycle, large differences arise. BFB risers have very low solids concentration in most of the furnace, being radiation the governing phenomena for heat transfer to the waterwalls. On the contrary, a large flow of solids flowing down by the walls make convection to be the governing mechanism in CFB units [1]. Very little work has been published regarding the comparison of performance of BFB and CFB boilers. One of the most detailed reviews to date was published by Koornneef et al. [2], who showed the commercial size limitation of BFB, which are thus mostly used for fuels with lower energy density, i.e. higher energy transport costs, such as biomass while CFB can profitably reach utility sizes. DeFusco et al. [3] presented a case study comparing BFB and CFB boilers for 50MW biomass combustion. It was suggested that a BFB unit would be more beneficial due to lower capital and operational cost as well as higher fuel flexibility. It was also stated that CFB units are the preferred option when fresh biomass is co-fired with higher heating value fuels (including low moisture fuels, such as urban waste wood).

Due to the high variability of fuel conditions (e.g. fuel mixture, moisture content or heating value of a certain fuel), it is crucial to understand transient operation of FBC units in order to design satisfactory control systems to keep the temperature field and heat transfer within operability limits. Additionally,

when commissioned in energy systems with currently increasing penetration of non-dispatchable generation of heat and power, fluidized bed boilers will be required to operate in cycling mode, stressing the need for fast and controlled load ramping, start-up and shut-down capabilities.

Dynamic modelling of the flue gas side of the boiler provides insight of the combustion process under varying operational conditions. The core purpose of dynamic models is to track key process variables over time, predicting their behaviour when a certain event or transition occurs. Furthermore, dynamic models are also used to test different control strategies and train operators. In addition, dynamic models of the gas side can be integrated into dynamic process models of the steam cycle, allowing the study of the dynamic interactions between both systems under transient operation.

Mathematical modelling of FBC units has been covered by many researchers for decades. However, the main focus has been on steady or quasi-steady state models (for semi-empirical and CFD modeling, respectively) that provide useful knowledge for the design and operation of FBC units around a given operating condition. There is considerably less work done regarding the area of dynamic modelling of FB boilers. Regarding CFB combustors, some authors have focused on the combustion dynamics [4], aiming to predict the residence time of solids and the char inventory over time. Park and Basu [5] aimed to predict the concentrations of char and oxygen after a fuel shift, presenting a model validated against a 0.3 MW unit. Chen and Xiaolong [6] published a dynamic model of a 410 t/h coal CFB unit, which was applied to resemble a certain dynamic operation of the boiler. Other authors have focused their efforts in developing dynamic models to design and test control structures, see [7] and [8]. When it comes to BFB units, the amount of published work is even more scarce. Kataja et al. [9] presented a dynamic model of a coal-fired BFB boiler which included both the flue-gas side and steam-water side, applying it to simulate a change in fuel feed and fuel moisture content. A similar model was presented by Selcuk et al. [10], which was validated against a 0.3 MW pilot plant. In summary, it is shown that there is a lack of knowledge when it comes to predict the dynamics of the gas side of fluidized bed boilers, especially when it comes to comparing the dynamic behaviour of bubbling and circulating fluidized bed combustors.

The aim of this work is to compare the transient behaviour of BFB and CFB boilers of the same size under given transient scenarios. For this, dynamic models of the gas side of FB combustors, both BFB and CFB units, are presented and used to simulate two industrial-sized (130 MW_{th}) conditions.

2. Models description

The models presented in this paper consist of an assembly of control volumes exchanging mass and energy. The models have some common features while some other aspects are specific of each application (BFB or CFB), as presented in sections 2.1 and 2.2. Figure 1 shows a schematic representation of the main control volumes and their connections for both models. It is seen that while some of the control volumes are used in both the BFB and CFB models (shown with solid line in Figure 1), others are exclusive to the CFB model (dotted lined elements in Figure 1). Similarly, the volumes in the furnace exchange gas flows in both models (black solid arrows) and also solid flows in the CFB model (red dotted arrows).

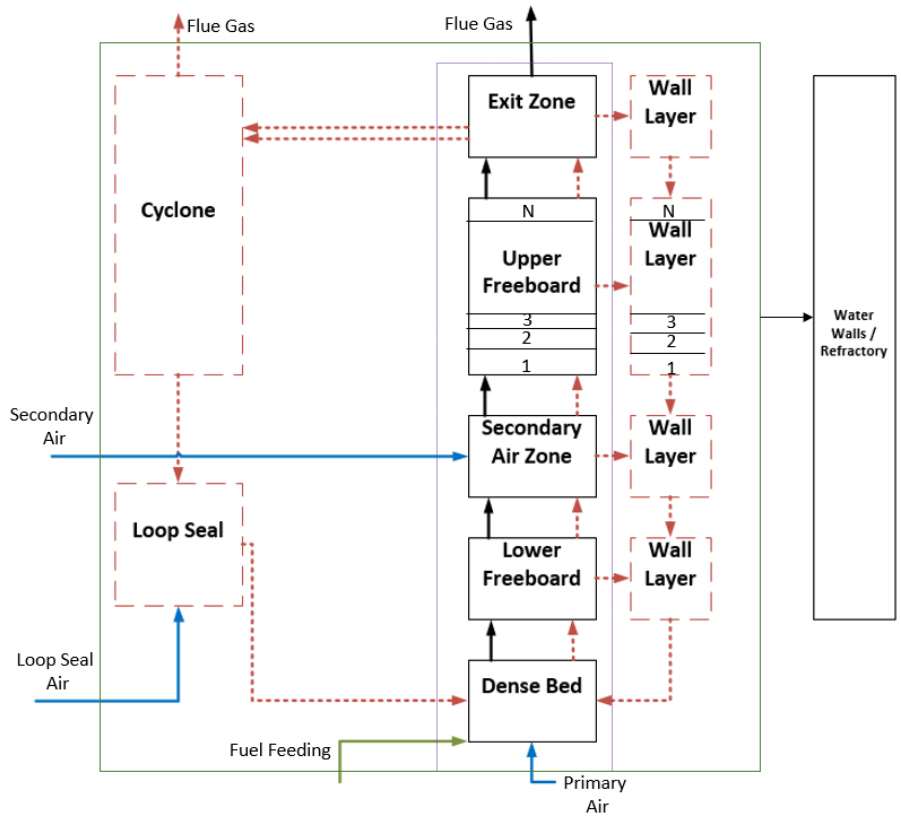

Figure 1. Schematic diagram of the model. Solid line elements are present in both BFB and CFB configurations, while dotted elements are only present in the CFB. The figure also shows the waterwalls and refractory as given temperature boundary condition.

The control volumes are modelled as continuously stirred tank reactors (CSTR), i.e. assuming perfect mixing inside the volume. Note that the regions that exhibit a plug-flow behaviour, e.g. the upper freeboard, are modelled as a consecution of *N* stirred tank reactors. Dynamic mass and energy balances are formulated in each of them, accounting for the three phases included in the model: bulk solids, fuel and gas. From these balances, the concentrations of all the species considered and the temperature is solved in each control volume.

Model inputs consist of boiler geometry, fed air and fuel flows, fuel composition, and boundary temperature in the waterwalls. As an output the model provides, in all the control volumes defined, the temperature, the heat flow transferred to the walls, and the concentrations and mass flows of solids, fuel classes and gas species.

Inert solids, whose addition and removal has been neglected, are characterized by a single class with the mean particle size. The fuel phase has been modelled as 3 conversion classes, to account for differences in density and particle size as conversion evolves. The gas phase accounts for nine species: H_2, O_2, CO, CO_2, H_2, H_2O, NH_3, H_2S and heavy hydrocarbons (tar). Three homogeneous reactions have been included (oxidation of carbon monoxide, hydrogen and tar) along with char oxidation; the kinetics are taken from [11] and [12]. The waterwalls are modelled as boundary conditions with a given constant temperature, T_w, which in this work is assumed to be equal to the waterside temperature. Refractory material can be present in some regions, in which the heat extraction is set to zero.

The key differences between the BFB and the CFB models are the mechanisms for heat transfer to the walls and solids hydrodynamics, whose modeling is described below.

2.1. Bubbling fluidized bed model

The bulk solids and fuel phases remain in the dense bed region, making radiation to be the dominating mechanism driving the heat transfer to the furnace walls. Radiative heat flows to and from each surface

inside the furnace (namely the dense bed surface, and the furnace sidewalls and roof) as well as from and to each gas volume. Equation 1 shows the heat balance over a certain surface *s*, and Equation 2 and 3 expand the values of heat received $q_{in,s}$ and emitted $q_{emitted,s}$.

$$q_{net,s} = \alpha_w q_{in,s} - q_{emitted,s} \quad (1)$$

$$q_{in,s} = \sum_j \left(\sigma \varepsilon_j T_j^4 + q_{in,j}\left(1-\varepsilon_j\right)\right) \cdot A_j F_{js} \prod_j^s (1-\alpha_{g,js})) + \sum_k \left(\sigma \varepsilon_{g,k} T_{g,k}^4 A_k F_{ks} \prod_k^s (1-\alpha_{g,ks})\right) \quad (2)$$

$$q_{emitted,s} = \sigma \varepsilon_w T_s^4 A_s \quad (3)$$

The first term of Equation 2 refers to the total incoming radiation from other surfaces within the furnace (i.e. other waterwalls or the bed surface). Note that this term consists of the emitted and reflected radiation of the surface *j*, multiplied by the view factor between surfaces *j* and *s* F_{js}, and by (1-α) of all the control volumes that the flux crosses from *j* to s, in order to account for the fraction that is absorbed by the gas. The second term of Equation 2 represents the gas radiation from the control volume *k* to the surface *s* (note that the gas absorption on the way from *k* to *s* has also been included). The view factors between surfaces and volume and surfaces have been computed according to [13].

Regarding the control volumes occupied by gas, a similar balance like the one showed in Equation 1 is applied. The heat flows emitted and received in a certain gas volume *g* are computed according to Equation 4 and 5.

$$q_{in,g} = \sum_j \sum_i \left(q_{emitted,j} A_j F_{ji} \prod_k^s \left(\left(1-\alpha_{k,ij}\right)\right) \alpha_g \right) + \sum_k \left(\sigma A_k F_{k,g} \varepsilon_k T_k^4\right) \prod_n^g (1-\alpha_n) + \sum_k \sum_i \left(\sigma \varepsilon_{g,k} A_k F_{ki} T_k^4 \prod_h^s \left(\left(1-\alpha_{h,ks}\right)\right) \alpha_g \right) \quad (4)$$

$$q_{emitted,g} = \sigma \varepsilon_g T_g^4 A_g \quad (5)$$

$$\varepsilon_g = 1 - e^{-k_g L} \quad (6)$$

The first term of Equation 4 refers to the absorbed radiation from surface to surface, in which the fraction absorbed by other gas volumes has also been accounted. The second term accounts for the gas to gas radiation while the third term includes the absorbed fraction from all the gas to surface radiation crossing the gas volume *g*. Equation 5 shows the emitted radiation of a gas element (which is equal to the sum of all the gas-gas and gas-surface radiation emitted from the volume *g*).

It is known that the freeboard of BFB boilers contains a small fraction of fine solids (whose mass is neglected in the model) which will increase the radiation absorbed and emitted by the control volume. Hence, since the amount of solids present in the gas at different heights is not known, the effective emissivity of the control volumes in the freeboard of the BFB is handled in the model as a calibration factor, where the value of the k_g in the expression for the Beer law is tuned, see Equation 6.

2.2. Circulating fluidized bed model

As shown in Figure 1, the CFB model presented in this work has a 1.5D representation of the furnace, i.e. it accounts for the core-annulus structure of the solids flow. The hydrodynamics of the solids have been implemented according to the model presented by Johnsson et al.[14]. The fraction of solids entrained from the dense bed by the gas flow is computed based on the data presented by Djerf et al. [15] and tuned with a pre-exponential factor. Some of these entrained solids are back-mixed through the furnace wall layers while the rest reach the exit region. The net transfer of solids from the core region to the wall-layers at different heights is modelled according to [16]. Finally, at the exit duct the solids experience a backflow effect, modelled based on data shown in [15]. Figure 2 illustrates a certain control volume in the riser, showing the flows of solids between core and wall-layer. The model neglects the presence of gas phase in the wall-layers.

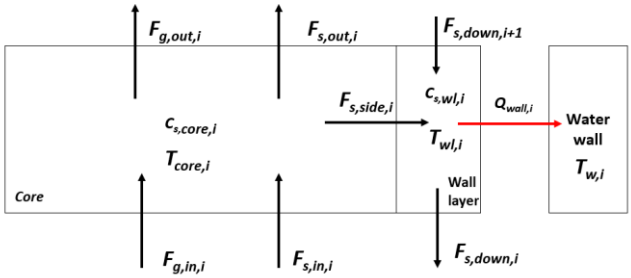

Figure 2. Schematic representation of the mass flows entering and exiting the control volumes at a certain height of the CFB furnace. The figure shows also concentrations and temperatures calculated in each volume. The water wall box acts as temperature boundary condition.

Equation 7 formulates the expression used to compute the heat transferred to the waterwalls at a certain height, where A is the heat exchange area assigned to the control volume i, h_c is the heat transfer coefficient (calculated according to Breitholtz et al. [1] and tuned afterwards) and ε is the average emissivity of the suspension and walls. Radiation is accounted as suggested by Breitholtz et al [1], i.e. a radiation efficiency η_{rad} has been included to account for the increase of radiation when the solids concentration at the wall layers decreases. Note that the temperature governing the radiative heat transfer is that at the core while the wall-layer temperature is used for the convective heat flow.

$$Q_{wall,i} = h_c \cdot A_i \cdot (T_{wl} - T_w) + \eta_{rad} \cdot \varepsilon \cdot A_i \cdot \sigma \cdot (T_{core}^4 - T_w^4) \qquad (7)$$

3. Model parametrization and validation

In order to validate the modeling for large-scale circulating and bubbling fluidized bed boilers, the models are parametrized using design and steady-state operational data from two industrial facilities: a 130 MW_{th} bubbling fluidized bed boiler (Övik Energy, Sweden) and a 80 MW_{th} circulating fluidized bed boiler (Karlstads Energi, Sweden). The main inputs to the models are shown in Tables 1 and 2.

The reference CFB unit has two cyclones and two loop seal systems, being the fuel fed in the return legs connecting the loop seals with the furnace. Secondary air is injected at a height of 5 m. The upper freeboard is discretized in N=10 control volumes. The reference BFB unit has secondary air injections at a height of 6 m and its upper freeboard is modelled through N=11 volumes. The bulk solids in both units are modelled as conventional silica sand for fluidized bed boilers, with. It is important to mention that both boilers have an additional heat removal inserted in the furnace apart from the waterwalls: the BFB unit has the tertiary superheater inserted in the furnace (starting at a height of 17 m) while the CFB boiler has a secondary superheater inserted at a height of 13 m. They both are modelled as heat sinks of 18 MW and 2.4 MW respectively, which remove the mentioned heat rates from the control volumes at the mentioned heights.

Table 1. List of design and operational data used as inputs

Parameter	BFB boiler	CFB boiler
Furnace Height	30 m	21 m
Furnace Width	9.18 m	8.50 m
Furnace Depth	8.67 m	4.1 m
Fuel flow	13.8 kg/s	12 kg/s
Air flow	38 Nm^3/s	30.6 Nm^3/s
Primary/Secondary air ratio	0.74	0.78
Recirculated flue gas flow	14 Nm^3/s	-
Waterwalls projected area	885 m2	425 m^2
Gas velocity	3.4 m/s	4.8 m/s
Air inlet temperature	260 ˚C	190 ˚C
Steam temperature	344 ˚C	290 ˚C
Cyclone volume	-	77.5 x 2 m^3

The fuel in both plants consists of a mixture of different biomass types that varies in frequently in composition. To simplify the study, both plants have been modelled with the same dry fuel composition (a biomass standard composition taken from [17]), but with differing moisture contents in order to match those under real conditions (the fuel in the BFB unit has 40% moisture while the CFB unit has 54%). Table 2 shows the proximate and ultimate analysis of the fuel fed to the models.

Table 2. Proximate (dry basis) and ultimate (dry-ash-free) analysis included in the model to simulate the BFB and CFB industrial boilers

Proximate Analysis (dry basis)	
Volatiles	78.26 wt%
Char	20.87 wt%
Ash	0.87 wt%
Ultimate Analysis (dry-ash-free)	
C	50.60 wt%
H	5.90 wt%
O	43.20 wt%
N	0.08 wt%
S	0.04 wt%

Table 3 lists the main validation results from the model after simulating the design load cases for both industrial units. The simulated process variables are compared with the operational data from the plants, measuring the deviations as relative or absolute error, depending on the variable. These deviations remain below 10% for all variables and exist due to inherent errors related to the measuring and modelling uncertainty.

Table 3. Model validation: comparison of measured and modeled values of the main process variables

CFB boiler				
Variable	**Unit**	**Measured**	**Modeled**	**Error**
Solids inventory in lower bed	kg	19200	18700	1.5 %
Solids inventory in upper bed	kg	6400	6000	6.2 %
Temp. dense bed	˚C	798	803	5 ˚C
Temp. lower freeboard	˚C	844	830	7 ˚C
Temp. secondary air injection	˚C	834	825	9 ˚C
Temp. close to superheater	˚C	839	840	1 ˚C
Temp. at riser exit	˚C	862	860	2 ˚C
Temp. at cyclone exit	˚C	880	890	10 ˚C
O_2 in exhaust gas	$\%_{vol}$	2.0	1.9	0.1 %-units
CO_2 in exhaust gas	$\%_{vol}$	16.3	15.6	0.4 %-units
H_2O in exhaust gas	$\%_{vol}$	33.5	32.0	1.0 %-units
Heat transferred to walls	MW	43.8	42.5	2.3%

BFB boiler				
Variable	**Unit**	**Measured**	**Modeled**	**Error**
Temp. dense bed	˚C	835	850	15 ˚C
Temp. before superheaters	˚C	1050	1035	15 ˚C
Temp. after superheaters	˚C	760	747	13 ˚C
O_2 in exhaust gas	$\%_{vol}$	2.5	2.8	0.3 %-units
CO in exhaust gas	$\%_{vol}$	0.0035	0.0045	0.0005 %-units
H_2O in exhaust gas	$\%_{vol}$	22	20.2	1.8 %-units
Heat transferred to walls	MW	59	60	1.60 %

4. Dynamic simulations

The model presented is applied to investigate the differences in transient behaviour between industrial BFB and CFB boilers. In order to establish a fair comparison and avoid effects related to the size of the unit, the CFB model is scaled-up to a 130 MW unit. After being validated with operational data from an 80 MW industrial unit, the model is parametrized again to resemble a larger unit with similar operational conditions: the cross-sectional area is increased in order to keep the gas velocity constant and the height of the furnace is increased to maintain the same concentration of solids at the top of the riser as the 80 MW reference unit. The superheater inserted in the furnace has its load increased in order to keep the same gas temperature at the furnace exit, while the air-to-fuel ratio and the primary-to-secondary air ratio are kept constant.

The scenarios simulated are a load reduction from 100% to 80% (keeping the air-to-fuel and primary-to-secondary air ratios constant) as well as a fuel moisture content increase by 10%. The open-loop (uncontrolled) responses of the units are evaluated by applying the changes mentioned before in the form of steps and measuring the stabilization time of the main process variables. The stabilization time t_s is computed as the time it takes for a certain process variable to do 10% of the total change after a certain variation is applied (see Equation 8, where y_∞ refers to the new steady-state value after the change and Δy is the absolute change in steady-state values before and after the change). The relative change RC of the variable once the new steady-state is reached is computed as shown in Equation 9. The process variables selected to perform the comparison are the temperature in the dense bed, T_{db}, the temperature at the top of the riser before the superheaters, T_{top}, and the heat transferred to the waterwalls, Q_{wall}.

$$y_\infty - 0.1\Delta y < y_\infty < y_\infty + 0.1\Delta y \qquad (8)$$

$$RC = 100 \cdot \frac{y_\infty - y_0}{y_0} \qquad (9)$$

5. Results and discussion

Figure 3 shows the resulting trajectories of the selected process variables when a step-down in load is introduced at t=0 (marked as a dotted line), whereas the trajectories when a step-up in fuel moisture is introduced are plotted in Figure 4. The stabilization times and relative changes of the variables of interest are listed in Table 4.

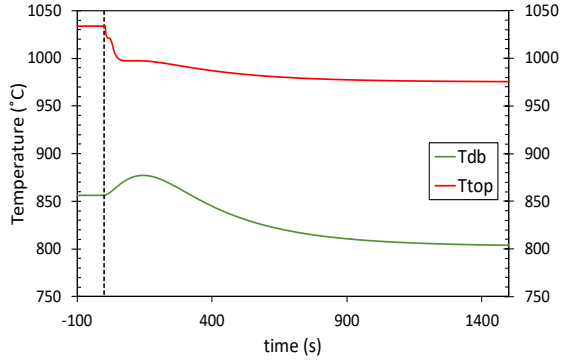

a) Simulated temperatures in dense bed and before superheaters in the BFB

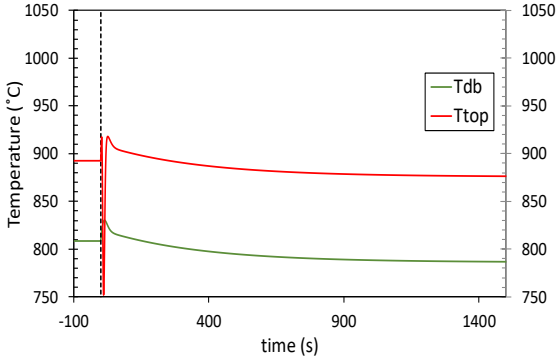

b) Simulated temperatures in dense bed and before cyclone in the CFB

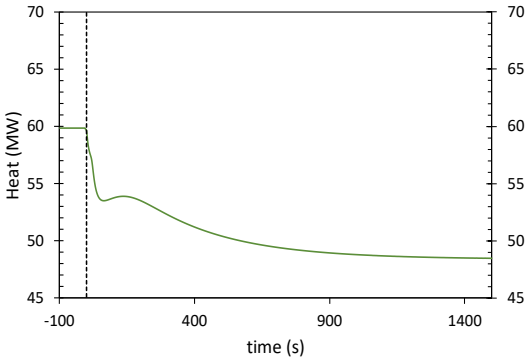

c) Simulated heat transfer to the waterwalls in the BFB

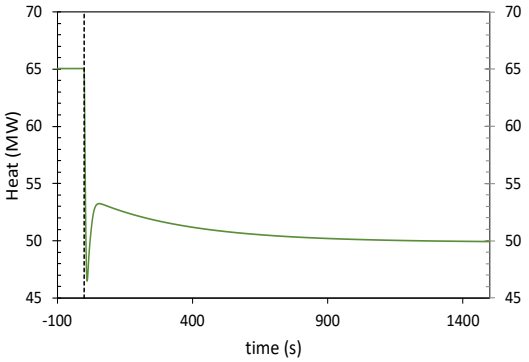

d) Simulated heat transfer to the waterwalls in the CFB

Figure 3. Transient responses of the relevant process variables after a 20% load reduction step change is introduced at t=0 (represented with dotted black line).

It can be observed in Figure 3b that the temperatures in the CFB unit exhibit inverse responses, both in the dense bed and the top of the riser. A similar response is observed in the dense bed of the BFB, whereas the BFB upper region does not show such behaviour. This indicates that the presence of solids is largely related to the observed inverse responses. As seen in Figure 3c, the heat transferred to the water walls drops slowly in the BFB boiler, reaching stabilization after 586 s. On the other hand, the CFB boiler shows a sudden drop in transferred heat followed by an increase and a slight decrease towards stabilization, reached after 333 s. As seen in Table 4, the difference in stabilization time is caused by the differences in relative change of the temperatures when a 20% load decrease occurs: due to the high thermal inertia of the CFB boiler the temperature change is smaller and the heat transfer reaches its new steady-state faster.

When a 10% step-up in fuel moisture content is simulated, the temperatures simulated in both CFB and BFB units fall smoothly towards their new steady-state values. In both boilers the dense bed presents a slower response than the top of the riser, caused by the fact that the drying of the fuel occurs in the dense bed, characterized by the presence of a large mass of solids. As seen in Table 4, relative changes in CFB variables are once again smaller than in the BFB and the heat transfer to the water side stabilizes faster. Another aspect that can be extracted from Figure 4 is the fact that no inverse response is observed in the CFB temperatures after a moisture change, which is in relation with what was stated above: the change in solids fluxes (dependant on gas velocity) are responsible for the inverse transients in the upper furnace.

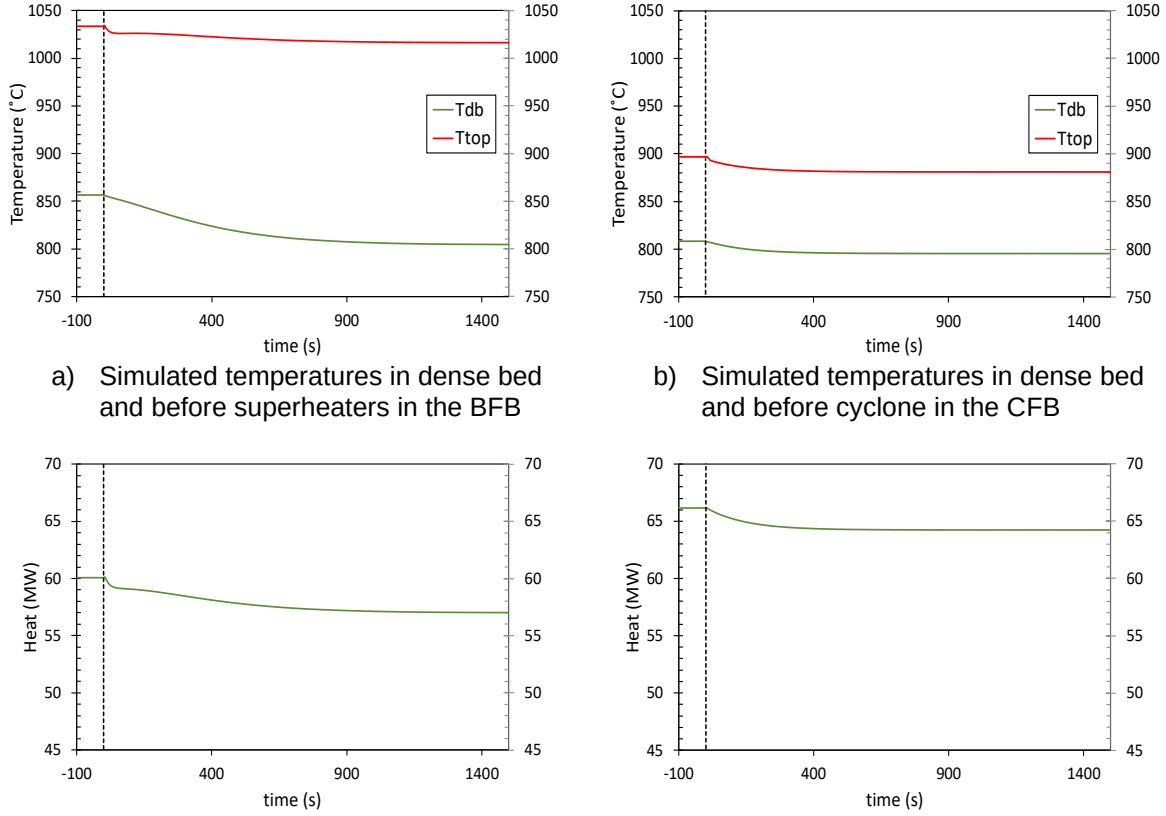

a) Simulated temperatures in dense bed and before superheaters in the BFB

b) Simulated temperatures in dense bed and before cyclone in the CFB

c) Simulated heat transfer to the waterwalls in the BFB

d) Simulated heat transfer to the waterwalls in the CFB

Figure 4. Transient responses of the relevant process variables after a 10% step increase in fuel moisture is introduced at t=0 (represented with dotted black line).

Table 4. Stabilization times and relative changes of the relevant process variables when a 20% load step-down and a 10% step-up in fuel moisture are introduced respectively.

	BFB			CFB		
Load reduction	T_{db}	T_{top}	Q_{wall}	T_{db}	T_{top}	Q_{wall}
t_s(s)	814	602	586	850	951	333
RC(%)	5.5	5.4	18.4	2.4	1.8	24.6
Moisture increase						
t_s(s)	752	630	606	337	308	336
RC(%)	6.1	1.8	5.0	1.6	1.8	2.9

6. Conclusions

Dynamic models of the flue gas side of large-scale bubbling and circulating fluidized bed boilers have been developed. The models have been parametrized with design data from two industrial units and the steady-state of the models has been validated against operational data. The models are applied to compare the dynamic behaviour of a BFB and a CFB combustors of the same size (80 MW_{th}). To do so, two different scenarios are investigated: a 20% step-down in load and a 10% step-up in fuel moisture are simulated, while the system is kept in open-loop (uncontrolled) and the evolution with time of the main process variables is analysed.

Results show that the heat transfer to the water-walls stabilizes faster in the CFB unit. Temperatures in the CFB are less affected by changes than in the BFB boiler, caused by the larger thermal inertia

inherent to the solids fluxes in the circulating system. The presence of solids along the furnace make the temperatures in the CFB exhibit an inverse response when a step in air velocity is introduced, something that does not occur in the BFB since the presence of solids is limited to the dense bottom bed.

References

[1] C. Breitholtz, B. Leckner, and A. P. Baskakov, “Wall average heat transfer in CFB boilers,” *Powder Technol.*, vol. 120, no. 1–2, pp. 41–48, 2001.

[2] J. Koornneef and M. Junginger, “Development of fluidized bed combustion — An overview of trends , performance and cost,” *Prog. Energy Combust. Sci.*, vol. 33, pp. 19–55, 2007.

[3] J. DeFusco, P. McKenzie, and W. Stirgwolt, “A Comparison of Fluid-Bed Technologies for Renewable Energy Applications,” in *Renewable Energy World Conference*, 2010.

[4] J. Saastamoinen, “Modelling of dynamics of combustion of biomass in fluidized beds,” *Therm. Sci.*, vol. 8, no. 2, pp. 107–126, 2007.

[5] C. K. Park and P. Basu, “A model for prediction of transient response to the change of fuel feed rate to a circulating fluidized bed boiler furnace,” *Chem. Eng. Sci.*, vol. 52, no. 20, pp. 3499–3509, 1997.

[6] Y. Chen and G. Xiaolong, “Dynamic modeling and simulation of a 410 t/h Pyroflow CFB boiler,” *Comput. Chem. Eng.*, vol. 31, no. 1, pp. 21–31, 2006.

[7] N. Zimmerman, K. Kyprianidis, and C.-F. Lindberg, “Waste Fuel Combustion: Dynamic Modeling and Control,” *Processes*, vol. 6, no. 11, p. 222, 2018.

[8] J. Findejs, V. Havlena, J. Jech, and D. Pachner, “Model based control of the circulating fluidized bed boiler,” *IFAC Proc. Vol.*, vol. 42, no. 9, pp. 44–49, 2009.

[9] T. Kataja, P. O. Box, F.- Tampere, P. O. Box, and F.- Tampere, “Dynamic Model of a Bubbling Fluidized Bed Boiler,” pp. 140–149.

[10] N. Selçuk and E. Degirmenci, “Dynamic Simulation of Fluidized Bed Combustors and its Validation Against Measurements Dynamic Simulation of Fluidized Bed Combustors and its Validation Against Measurements,” vol. 2202, 2007.

[11] Flagan;Seinfeld, *Fundamentals of air pollution engineering*. Prentice Hall, 1988.

[12] F. L. Dryer and C. K. Westbrook, “Simplified Reaction Mechanisms for the Oxidation of Hydrocarbon Fuels in Flames,” *Combust. Sci. Technol.*, vol. 27, no. 1–2, pp. 31–43, 1981.

[13] Incropera;, DeWitt;, Bergman;, and Lavine, *Fundamentals of heat and mass transfer*, 6th ed. Wiley, 2007.

[14] F. Johnsson, W. Zhang, and B. Leckner, “Characteristics of the formation of particle wall layers in CFB boilers,” in *2nd Int. Conf. on Multiphase Flow, Vol 3*, 1995.

[15] T. Djerf, D. Pallarès, and F. Johnsson, “Evaluation of the fluid-dynamically down-scaled model of a 200 MWth CFB boiler,” in *Fluidization XVI*, 2019.

[16] F. Johnsson and B. Leckner, “Vertical distribution of solids in a CFB-furnace,” in *13th International conference on fluidized-bed combustion*, 1995, p. 719.

[17] T. R. Miles, T. R. J. Miles, L. . Baxter, R. Bryers, B. . Jenkins, and L. Oden, “Alkali deposits found in biomass power plants: a preliminary investigation of their extent and nature,” *Natl. Renew. Energy Lab.*, 1995.